Imaging subcellular features of a sectioned rat brain using time-of-flight secondary ion mass spectrometry and scanning probe microscopy

H.-Y. Nie [a,*], J.T. Francis [a], A.R. Taylor [b], M.J. Walzak [a], W.H. Chang [a], D.F. MacFabe [b], W.M. Lau [a]

[a] Surface Science Western, Room G-1, WSC, The University of Western Ontario, London, Ontario N6A 5B7, Canada
[b] The Kilee Patchell-Evans Autism Research Group, Departments of Psychology and Psychiatry, Division of Developmental Disabilities,
Shulich School of Medicine and Dentistry, The University of Western Ontario, Room 7252, SSC, London, Ontario N6A 5C2, Canada

ARTICLE INFO

ABSTRACT

Coronal sections of unfixed rat brain samples were prepared on a flat substrate in order to reveal hippocampal formation (CA1-4 pyramidal neurons) and adjacent neocortical white matter. We demonstrate the feasibility of using surface sensitive techniques such as time-of-flight secondary ion mass spectrometry (ToF-SIMS) and scanning probe microscopy (SPM) to probe lipid distribution, as well as the subcellular features of neurons. In the same anatomical areas, the phase shift image in SPM is especially useful in revealing the cross-section of subcellular structures. We show that the phase shift images reveal distinctive subcellular features and ion images of CN^- and PO_2^- fragments from ToF-SIMS appear to define some of the subcellular features.

1. Introduction

Time-of-flight secondary ion mass spectrometry (ToF-SIMS) is a powerful analytical technique to study the surface of organic molecules on a substrate with high mass resolution spectra combined with imaging capacity [1]. The imaging capacity is especially useful for the study of biological samples because it answers not only the question of what is on the surface but also the question of how those molecules are distributed on that surface. Imaging ToF-SIMS has been widely applied to biological samples such as sectioned animal brains and single cells [2–10]. For example, Sjövall et al. have imaged sectioned mouse brains, showing the distribution of cholesterol in the white matter area and other important component molecules such as phospholipids in discrete brain anatomical regions [4]. Richter et al. have investigated spatial localization of fatty acids on sectioned biological tissues such as rat cerebellum and mouse intestine [9]. ToF-SIMS has also been applied to study the structure of single cells such as thyroid tumor cells [10] and J774 cells [11] with a size range of 55–65 and ∼40 μm, respectively. Thus, ToF-SIMS has proven to be an extremely powerful technique to simultaneously measure and localize multiple diverse biochemical markers in biological systems.

The hippocampal formation of the brain is an ideal test region for ToF-SIMS imaging. An extensively studied neuroanatomical structure, it is believed to play an essential role in diverse cognitive processes, including spatial recognition, social behaviour and the formation and consolidation of memory. Large pyramidal neurons are easily localized within the structure, while nearby white matter tracts are enriched with non-neuronal cells (i.e. astrocytes and myelin containing oligodendroglia), which have a comparatively higher lipid content. The hippocampal formation is affected in a number of disorders including cerebrovascular disease, epilepsy, Alzheimer disease as well as a number of neurodevelopmental conditions. Regarding the later, MacFabe et al. recently found reversible behavioural and electrographic effects coupled with innate neuroinflammatory changes following intraventricular infusions of propionic acid; this has been proposed as a novel model of autism spectrum disorders [12,13]. This study used traditional immunohistochemical and biochemical techniques to examine increased oxidative stress and visualize neurons, reactive astrocytes, and activated microglia in hippocampus and adjacent external capsule white matter from coronally sectioned rat brain. In order to further visualize potential structural and metabolic changes induced by propionic acid infusion, we have recently started to use ToF-SIMS to map molecular distribution of a variety of bioactive compounds on sectioned rat brains.

In this paper, the initial ToF-SIMS results are presented from the hippocampal area using unfixed, sectioned brain samples from control rats [12]. In particular, it is demonstrated that organelle-

---

like features within a putative pyramidal neurons (~15 μm across in sectioned samples) may be visualized by specific ion fragments. We applied scanning probe microscopy (SPM), especially its phase shift [14–17] imaging technique to probe the subcellular features. The phase shift image, which is measured simultaneously with the topographic image, arises from the phase lag between the applied voltage source used to oscillate the cantilever and the actual oscillation of cantilever detected by the photodetector. The phase shift image is especially useful in revealing the cross-section of organelles having different mechanical properties. We show that the phase shift images reveal distinctive subcellular features with nanometer-scale resolution, thus providing a road map for ToF-SIMS imaging in exploring the molecular distribution within a cell. We report for the first time our results on subcellular features imaged at the same spot on a sectioned rat brain using both SPM and ToF-SIMS. We demonstrate that the combination of the two surface sensitive techniques provides new information on investigation of subcellular features.

2. Materials and methods

Adult male Long-Evans rats were sacrificed either by decapitation, or transcardiac perfusion with ice cold 2% paraformaldehyde under Nembutal anesthesia 0.1 M phosphate buffered saline (pH 7.5) using standard techniques [12]. Procedures were completed in accordance with guidelines of the Canadian Council on Animal Care (CCAC) and approved by the University of Western Ontario Animal Use Committee. Unfixed brains were rapidly removed and immediately frozen at −70 °C with OCT-embedding for cryoprotection. Coronal sections of dorsal hippocampus (5–30 μm) and adjacent neocortex and external capsule white matter were cut from the OCT-embedded brains in a cryostat operated at −20 °C and were placed on positively charged glass slides. Those sectioned rat brain samples on a glass slide were exposed to the ambient air and immediately subjected to SPM and/or ToF-SIMS analysis. For SPM measurements, the samples were used without being subjected to any drying process. On the other hand, for ToF-SIMS experiments, the samples were analyzed in vacuum, in which the samples were dried due to removal of moisture from the tissue.

An ION-TOF (Gmbh) TOF-SIMS IV equipped with a Bi liquid metal ion source was employed in this study. A 25 keV Bi_3^+ cluster primary ion beam pulsed at 10 kHz with a pulse width of 12 ns with a target current of 1 pA was used to probe large area. This high current bunched mode, providing a high mass resolution and strong secondary ion intensity, was used to probe fragments from important molecules in the brain, such as phosphocholine lipids and cholesterol. On the other hand, in order to obtain high spatial resolution, a 25 keV Bi^+ primary ion beam pulsed at 10 kHz with a pulse width of 170 ns with a target current of 0.01 pA was used for imaging CA1-4 (Cornu Ammonis) pyramidal neurons. This burst alignment mode, though low in secondary ion intensity, had a submicrometer spatial resolution. The secondary ions were extracted from the sample surface, mass separated and detected via a reflectron type of time-of-flight analyzer. In this study, only the negative secondary ion spectra were collected. A pulsed, low energy (18 eV) electron flood was employed to neutralize sample charging; the current was maintained below ~20 μA maximum to avoid sample damage. For both imaging modes, ion images were rendered by plotting their intensity against the pixels where mass spectra were collected.

A Park Systems XE-100 SPM was used to image one of the samples, prior to ToF-IMS imaging, in dynamic force mode, in which the cantilever with a spring constant of 40 N/m was oscillated and its amplitude was used as the feedback parameter to image the surface morphology and the phase shift contrast simultaneously with the topographic image. The phase shift image arises from the phase lag between the voltage source used to oscillate the bimorph on which the cantilever is attached and the actual oscillation of the cantilever as detected by the photodiode detecting system. The degree of phase lag is a measure of sample properties causing different interaction between the tip and the sample surface. The phase shift measured in our instrument at setpoint (i.e., when the tip was engaged to the sample surface at a working distance) was referred to that when the tip was in free space.

3. Results and discussion

Shown in Fig. 1 are negative ion mass/charge (m/z) spectra obtained on an area of 3.3 mm × 5.0 mm in the left hand side of the coronal section of the rat brain including hippocampal formation and adjacent neocortex and white matter. A number of fragments with biological significance relevant to rat brain have been assigned. For example, CN^- (nominal m/z = 26 amu) and CNO^- (42) are characteristic for nitrogen-containing molecules, including but not limited to proteins and nucleic acids. PO_2^- (63), PO_3^- (79) and $PO_4H_2^-$ (97) are the three major fragments for phosphate containing molecules such as cytoskeletal structural proteins, nucleic acids and phospholipids (a major component of cell and organelle membranes). $CH_3PO_4^-$ (110), $C_2H_4PO_4^-$ (123), $NC_2H_4PO_4^-$ (137) are fragments from the polar headgroup of phospholipids. $CH_4NC_2H_4PO_4^-$ (153) and $C_3H_8NC_2H_4PO_4^-$ (181) are believed to originate from phospholipids having the phosphocholine headgroup such as phosphatidylcholine, which were confirmed by a reference sample of purified phosphatidylcholine (DPPC). Those fragments may also be derived from sphingomyelin, a sphingolipid rich in neuronal plasma membranes, as it has the same phosphocholine headgroup.

$C_{16}H_{31}O_2^-$ (255), $C_{18}H_{33}O_2^-$ (281) and $C_{18}H_{35}O_2^-$ (283) are assigned to fatty acids palmitate, oleate, and stearate, respectively. Those fatty acids usually originate from the double chains of
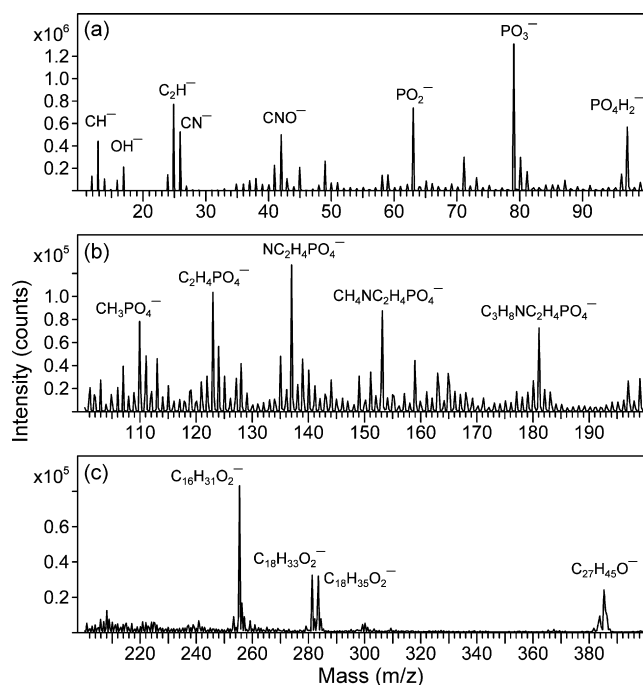

Fig. 1. Negative secondary ion mass spectra obtained using a Bi_3^+ primary beam on a sectioned rat brain film (thickness: 5 μm) in an area of 3.3 mm × 5 mm including the neocortex, white matter and hippocampal formation areas.

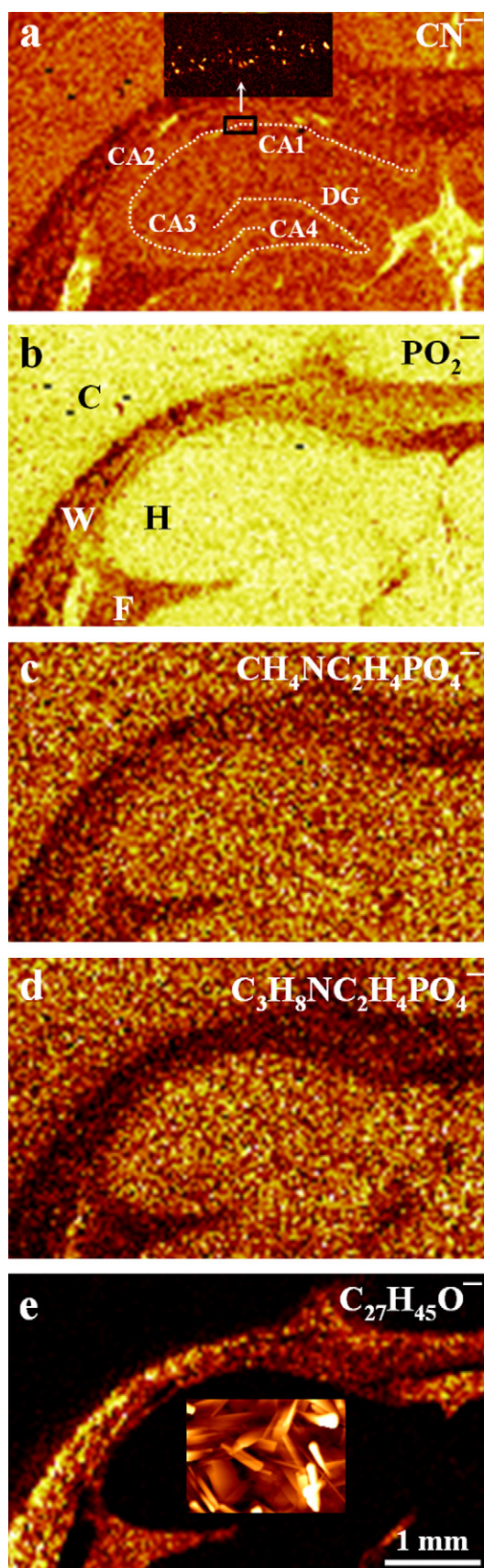**Fig. 2.** Negative secondary ion images (3.3 mm × 5.0 mm) of (a) CN^-, (b) PO_2^-, (c) $CH_4NC_2H_4PO_4^-$, (d) $C_3H_8NC_2H_4PO_4^-$ and (e) $C_{27}H_{45}O^-$ obtained on a sectioned rat brain film (thickness: 5 μm) using the high current bunched mode with the Bi_3^+

phospholipids found in animal brain. $C_{27}H_{45}O^-$ (385) is assigned to deprotonated cholesterol molecule, which is characteristic for the white matter area, as shown in Fig. 2e.

The imaging capacity of ToF-SIMS provides us information on where the fragments distribute over the sample surface. Shown in Fig. 2 are (a) CN^-, (b) PO_2^-, (c) $CH_4NC_2H_4PO_4^-$, (d) $C_3H_8NC_2H_4PO_4^-$ and (e) $C_{27}H_{54}O^-$ ion images for the scanned area. The data were collected from one scan of the sample (stage) with 128 shots per pixel on the 128 × 128 pixels over the area via the stage scanning mechanism. As shown in Fig. 2a, CN^- is relatively strong all over the surface, probably because it originates from all nitrogen-containing molecules. However, our intensive ToF-SIMS investigation on neurons concentrated in the CA1-4 and DG (dentate gyrus) fields suggests that neurons have a stronger CN^- signal than the surrounding area for an unfixed rat brain. Therefore, CN^- (as well as CNO^-) can be used as a contrast making fragment for identifying neurons on a sectioned brain sample surface.

In Fig. 2a, the CN^- contrast for the CA and DG fields (guided by the inserted dotted lines) is faint because the distance between two adjacent pixels is 39 μm in the image, while the neuron size is ~15 μm across for sectioned rat brain samples. Reducing the scan size should enhance the visualization of the neurons. For example, the inserted image (153 μm × 306 μm) in Fig. 1a is part of the CA1 field indicated by the inserted rectangle, where neurons are clearly revealed by CN^- contrast. This inserted image was obtained with the high spatial resolution (burst alignment) mode, in which the distance between the two adjacent pixels becomes 2.4 μm.

The letters C, W, F and H in Fig. 2b identify the neocortex, white matter, fimbria and hippocampal areas, respectively. PO_2^- seems to distribute evenly over the surface of the neocortex and hippocampal areas, but appears to be weaker in the white matter and fimbria areas. As PO_2^- should originate from any phosphate-containing molecules such as phospholipids and nucleic acids, its weaker signal in the white matter area suggests the existence of other molecules that are free of phosphate (as seen in Fig. 2e, cholesterol molecules are present on the white matter area). Shown in Fig. 2c and d are ion images for two of the many possible fragments originating from the phospholipidcholine headgroup, $CH_4NC_2H_4PO_4^-$ and $C_3H_8NC_2H_4PO_4^-$, respectively. It is clear that the white matter area has less phospholipidcholine content than do the neocortex and the hippocampal areas.

Fig. 2e shows the dominant presence of cholesterol in the white matter [4] and fimbria areas, indicating that the surface of the regions is enriched with cholesterol. In fact, as shown in the inserted image in Fig. 2e, the SPM topographic image collected in the white matter area of the external capsule clearly shows needle-like and flake-like features, suggesting that the white matter area is covered by cholesterol crystals. This is consistent with the comparatively higher levels of this molecule in the lipid membranes of axons and myelin containing oligodendroglia which comprise a major portion of this structure. The observed formation of crystalline cholesterol by SPM on the white matter area suggests that cholesterol molecules are highly mobile. While cholesterol is a major component of cell membrane, there is little cholesterol detected away from the white matter and fimbria areas at room temperature. It is apparent that cholesterol molecules would be highly diffusive at room temperature in vacuum if they were not crystallized.

primary ion beam. The dotted lines in (a) guide the eye to the CA1-4 and DG fields. In the CA1 field indicated by the inserted rectangle, there are neurons as shown in the inserted image (153 μm × 306 μm) which was obtained using the burst alignment mode. The letters C, W, F and H in (b) indicate the neocortex, white matter, fimbria and hippocampal formation areas, respectively. The inserted image in (e) is an SPM topographic image (22 μm × 28 μm) obtained on the white matter area.

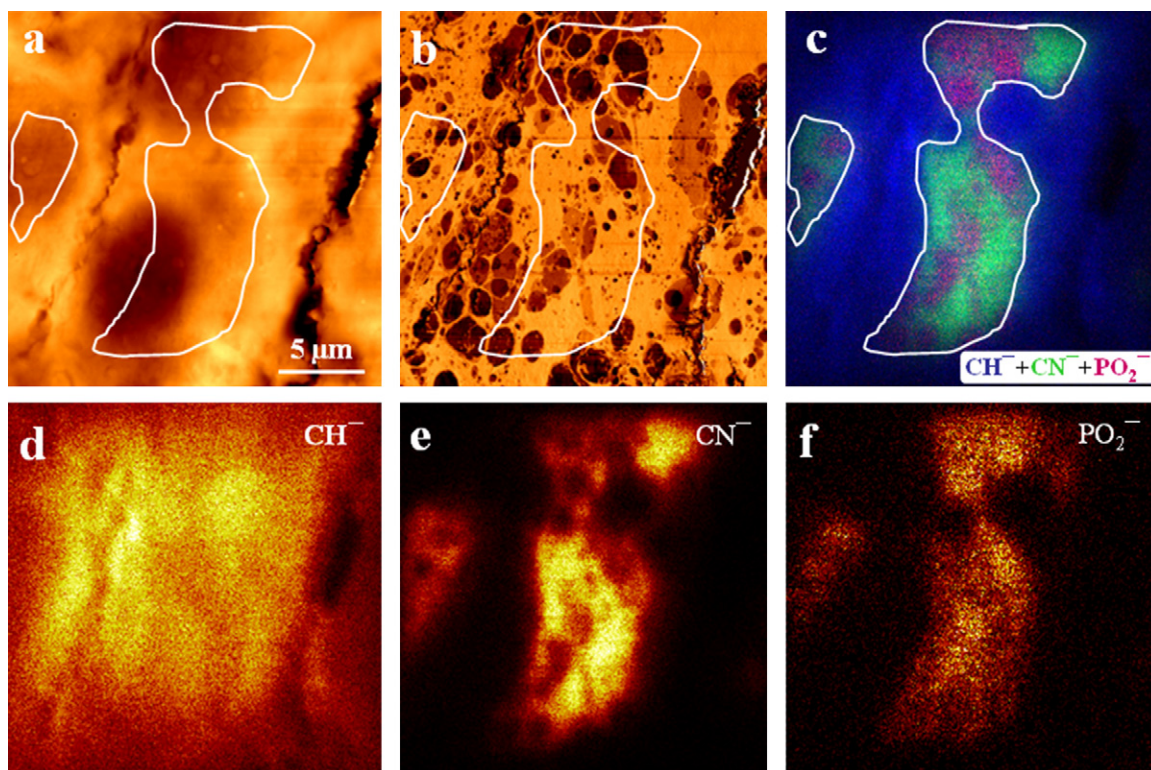**Fig. 3.** SPM topographic (a) and phase shift (b) images (22 μm × 22 μm) for neurons in the CA1 field obtained on a sectioned rat brain film (thickness: 30 μm). The ToF-SIMS negative secondary ion images of (d) CH^-, (e) CN^- and (f) PO_2^- are overlapped in (c) where CH^- is plotted in blue, CN^- in green and PO_2^- in red, respectively. The ion images were measured using Bi^+ primary ion beam with the high spatial resolution (burst alignment) mode. The ion images are plotted using 600 scans of data collection. The white lines inserted in (a)–(c) guide the eye to subcellular features imaged by both techniques. (For interpretation of the references to color in this figure legend, the reader is referred to the web version of the article.)

In order to investigate the feasibility of ToF-SIMS imaging on subcellular features on sectioned rat brain samples, SPM measurements on neurons in the CA1 field were first conducted because SPM has ample spatial resolution to reveal subcellular features. Shown in Fig. 3a is a topographic image obtained in the CA1 field of a separate sample, which had not been subjected to any drying process, at a location similar to that shown in the rectangle in Fig. 2a, where there is a band of neurons. The surface of unfixed sectioned rat brain samples appears to have cracks and depressions. For example, the depression seen in Fig. 3a is ∼6 μm wide and ∼300 nm deep. Other than the cracks and depressions observed on the surface of the sectioned sample, one can only extract limited information on revealing subcellular features from the topographic image alone. The subcellular structures are apparently obscured by the dynamic height range as determined by the cracks and depressions.

The phase shift image (Fig. 3b), on the other hand, shows striking contrasts in phase shift on the surface. The phase shift image shows reduced phase shift spots compared to the featureless area. Referring back at the topographic image (Fig. 3a) with the help of the phase shift image (Fig. 3b), one can now extract more information on the subcellular structures, which have a size range of 150 nm to 3 μm. A careful comparison of the two images reveals that some of the reduced phase shift spots in Fig. 3b correspond to raised features in Fig. 3a; while some of the reduced phase shift spots show no apparent morphological significance. We tentatively assign the reduced phase shift spots in Fig. 3b to organelles because of their sizes and shapes. Therefore, it is clear that phase shift image is especially useful in revealing subcellular features from their surroundings on unfixed rat brain films, most likely by way of a difference in mechanical properties. However, to relate the phase shift contrast to material properties [17], more work is needed in order to establish appropriate experimental conditions such as selection of setpoint and control of surface chemistry of the tip apex.

The burst alignment mode ion images obtained on the same location of the same sample after the SPM measurement are shown in Fig. 3c–f. CH^-, CN^- and PO_2^- ion images are shown in Fig. 3d–f, respectively. Because of the weak secondary ion intensity in the burst alignment mode, the data were collected 600 scans on 256 × 256 pixels with 1 shot per pixel over an area of 22 μm × 22 μm. Accumulating enough scans for sufficient signal strength is necessary to probe small features such as cells, when using the high spatial resolution imaging mode [10]. The weaker signal intensity at the edge of the scanned area shown in Fig. 3d is believed to be an artifact.

Fig. 3c is an overlay of three ion images with CH^- plotted in blue, CN^- in green and PO_2^- in red. This overlaid image shows that CN^- and PO_2^- are more or less anti-coincident. It is interesting to note that in Figs. 3c, e and f, CN^- and PO_2^- fragments appear to correspond to features in the reduced phase shift image shown in Fig. 3b. To be more specific, the reduced phase shift spots seem to have lower CN^- intensity and higher PO_2^- intensity. The smallest spot size that shows phase shift contrast (Fig. 3b) and is evident in the CN^- and PO_2^- (Fig. 3c) ToF-SIMS images is ∼700 nm in diameter. Those fragments could originate from proteins and phospholipids or many other types of molecules. The reduced phase shift spots in Fig. 3b have stronger PO_2^- signals as shown in Fig. 3c and f, suggesting possible existence of organelles having concentration of phosphate-containing molecules such as DNA and RNA. It is also apparent that those features are surrounded by strong CN^- signals, hinting possible presence of proteins.

It is quite intriguing that the spots showing phase shift contrasts, outside the areas surrounded by the inserted lines, are dominated by CH^-, the reason for which remains unclear. Nevertheless, our SPM and ToF-SIMS images demonstrate the capabilities of those two techniques in revealing subcellular features for biological samples. These results are intriguing enough to warrant further investigations of SPM and ToF-SIMS imaging of subcellular features in sectioned rat brain samples.

Because the surface was prepared by microtome sectioning, identification of the observed features needs more work such as comparison to traditional histochemical techniques capable of identifying specific organelles. Of course at this preliminary stage, it is impossible to determine the exact identification of the subcellular structures observed. The sizes, however, are consistent with various organelles such as mitochondria, peroxisomes, vacuoles, endoplasmic reticulum and Golgi apparatus. Future studies comparing this technique with other standard histological techniques (i.e., transmission electron microscopy and immuno-histochemistry) to confirm the identification of these structures will be necessary.

4. Conclusions

We have imaged unfixed sectioned rat brain film samples, concentrated on the hippocampal formation and neocortical white matter area, using ToF-SIMS to study the spatial distributions of phosphocholine lipid and cholesterol. Phase shift contrasts imaged by SPM and CN^- and PO_2^- contrasts imaged by ToF-SIMS on the same location of neurons in the hippocampal formation demon-strated that it is feasible for those two techniques to image subcellular features in neurons. We emphasize that because SPM possesses a much higher spatial resolution and its phase shift imaging is especially useful in revealing subcellular features, it serves as a road map for ToF-SIMS in revealing subcellular features on sectioned biological tissues.

Acknowledgement

References

[1] A. Benninghoven, Angew. Chem. Int. Ed. Engl. 33 (1994) 1023.
[2] D. Léonard, H.J. Mathieu, Fresenius J. Anal. Chem. 365 (1999) 3.
[3] A.M. Belu, D.J. Graham, D.G. Castner, Biomaterials 24 (2003) 3635.
[4] P. Sjövall, J. Lausmaa, B. Johnasson, Anal. Chem. 76 (2004) 4271.
[5] D. Touboul, F. Kollmer, E. Niehuis, A. Brunelle, O. Laprévote, J. Am. Soc. Mass Spectrom. 16 (2005) 1608.
[6] A. Brunelle, D. Touboul, O. Laprévote, J. Mass Spectrom. 40 (2005) 985.
[7] K. Börner, P. Malmberg, J.-E. Månsson, H. Nygren, Int. J. Mass Spectrom. 260 (2007) 128.
[8] K.R. Amaya, E.B. Monroe, J.V. Sweedler, D.F. Clayton, Int. J. Mass Spectrom. 260 (2007) 121.
[9] K. Richter, H. Nygren, P. Malmberg, B. Hagenhoff, Microsc. Res. Techniq. 70 (2007) 640.
[10] H. Nygren, B. Hagenhoff, P. Malmberg, M. Nilsson, K. Richter, Microsc. Res. Techniq. 70 (2007) 969.
[11] S.G. Ostrowski, M.E. Kurczy, T.P. Roddy, N. Winograd, A.G. Ewing, Anal. Chem. 79 (2007) 3554.
[12] D.F. MacFabe, D.P. Cain, K. Rodriguez-Capote, A.E. Franklin, J.E. Hoffman, F. Boon, A.R. Taylor, M. Kavaliers, K.-P. Ossenkopp, Behav. Brain Res. 176 (2007) 149.
[13] D.F. MacFabe, K. Rodríguez-Capote, J.E. Hoffman, A.E. Franklin, Y. Mohammad-Asef, A.R. Taylor, F. Boon, D.P. Cain, M. Kavaliers, F. Possmayer, K.-P. Ossenkopp, Am. J. Biochem. Biotechnol. 4 (2008) 146.
[14] J. Tamayo, R. García, Langmuir 12 (1996) 4430.
[15] S.N. Magonov, V. Elings, M.-H. Whangbo, Surf. Sci. 375 (1997) L385.
[16] J.P. Cleveland, B. Anczykowski, A.E. Schmid, V.B. Elings, Appl. Phys. Lett. 72 (1998) 2613.
[17] N.F. Martínez, R. García, Nanotechnology 17 (2006) S167.